Article

The Speed of Evolution and Maintenance of Variation in Asexual Populations

Michael M. Desai,[1,2,5,*] **Daniel S. Fisher,**[1,3]
and Andrew W. Murray[2,4]
[1] Department of Physics
[2] Department of Molecular and Cell Biology
[3] Division of Engineering and Applied Sciences
[4] Bauer Center for Genomics Research
Harvard University
Cambridge, Massachusetts 02138

Summary

Background: The rate at which beneficial mutations accumulate determines how fast asexual populations evolve, but this is only partially understood. Some recent clonal-interference models suggest that evolution in large asexual populations is limited because smaller beneficial mutations are outcompeted by larger beneficial mutations that occur in different lineages within the same population. This analysis assumes that the important mutations fix one at a time; it ignores multiple beneficial mutations that occur in the lineage of an earlier beneficial mutation, before the first mutation in the series can fix. We focus on the effects of such multiple mutations.
Results: Our analysis predicts that the variation in fitness maintained by a continuously evolving population increases as the logarithm of the population size and logarithm of the mutation rate and thus yields a similar logarithmic increase in the speed of evolution. To test these predictions, we evolved asexual budding yeast in glucose-limited media at a range of population sizes and mutation rates.
Conclusions: We find that their evolution is dominated by the accumulation of multiple mutations of moderate effect. Our results agree with our theoretical predictions and are inconsistent with the one-by-one fixation of mutants assumed by recent clonal-interference analysis.

Introduction

How do the mutation rate, population size, and the magnitude of beneficial mutations determine the rate at which asexual populations evolve? This question is important for comparing among different experimental populations and with natural populations, as well as for understanding the effects of factors that could increase the rate of evolution such as sex [1–10] or mutator phenotypes [6, 11–15]. Lenski and others have found that, above a certain size, laboratory asexual populations do not evolve more quickly at large population sizes and mutation rates than at small ones [4, 16–19]. Their work is consistent with recent "clonal-

interference" theories of asexual evolution, in which the speed of evolution is limited in large populations because most beneficial mutations that occur in other lineages in the same population [20–26]. However, these experiments did not monitor the distributions of fitnesses within populations as they evolved, and these distributions are important in discriminating between different theories.

We have measured the speed of evolution and the distribution of fitnesses in evolving asexual populations of budding yeast at a range of population sizes and two mutation rates. Our results are inconsistent with recent clonal-interference analyses. Rather, they agree with theoretical predictions that the speed of evolution in large populations is dominated by multiple mutations that occur in the same lineage before the first mutation in the series has fixed. These mutations piggyback on each other in the sense that the presence of one beneficial mutation in a lineage helps another mutation in that lineage to outcompete other beneficial, same-sized mutations that occur in other lineages that have fewer or smaller beneficial mutations. The balance between clonal interference and multiple mutations sets the typical size of the mutations that accumulate on top of one another.

Theory

Theories for the evolution of asexual populations come in three flavors. The first applies to small populations. If the effective size of a population is N and the beneficial mutation rate is U_b, then new beneficial mutations arise at a rate NU_b. Most of these mutations are lost by genetic drift before they become abundant enough to reliably prosper. But for a mutation with a selective advantage s, there is a probability s that the mutant lineage will survive drift and grow common enough for its selective advantage to take over. We call this *establishment* of the mutant population (More generally, there is a probability As that a mutant lineage will survive drift, where A is a constant of order 1 that depends on the specific stochastic model of the dynamics [27]; our results are based on a continuous-time branching process model where $A = 1$, but the value of A is unimportant in the analysis presented here.). If nothing else interferes, mutations that establish will eventually outcompete and eliminate the genotype that gave rise to them. The time it takes a mutant to get from establishment to being half of the population is approximately $\frac{1}{s}\ln[Ns]$, whereas the time between the establishment of successive mutations is $\frac{1}{NU_b s}$. Thus, when $NU_b \ll \frac{1}{\ln[Ns]}$, mutations fix much more rapidly than they are established and thus evolution is mutation limited. The rate of evolution v—defined as the rate of change of the mean fitness (more precisely, the mean log fitness) of the population—is $v \approx NU_b \langle s^2 \rangle$, where $\langle s^2 \rangle$ is the mean square s. This is known as the one-locus regime (sometimes called the strong-selection weak-mutation regime); to

*Correspondence: mmdesai@princeton.edu
[5] Present address: Lewis-Sigler Institute for Integrative Genomics, Princeton University, Princeton, New Jersey 08544.
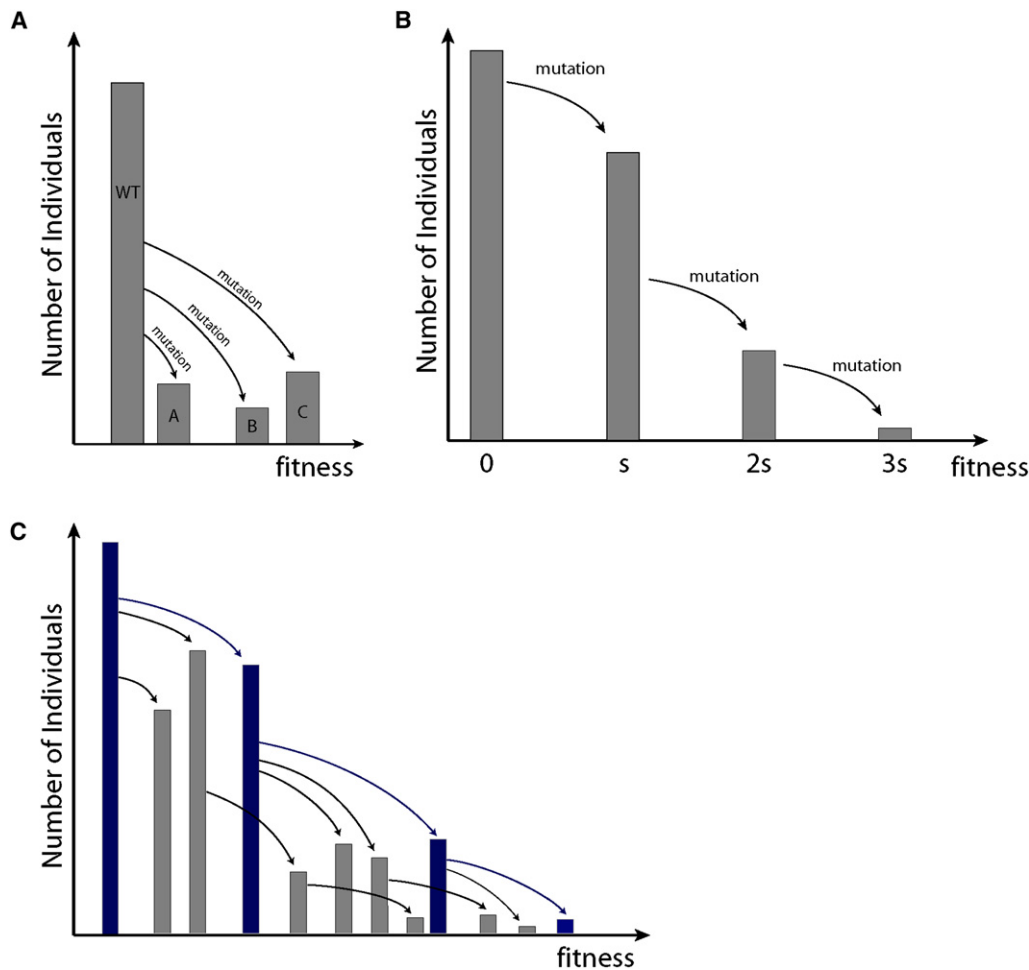
Figure 1. Schematics of One-by-One Clonal Interference and Multiple-Mutations Analyses

(A) One-by-one clonal interference. A population (the original wild-type [WT]) gives rise to several different beneficial mutations, which must compete. Here, mutation C will eventually outcompete A and B, causing these beneficial mutations to be "wasted." The theory then assumes that C fixes and becomes the new WT, and the process repeats. Additional mutations that happen in A, B, or C before C fixes are neglected.

(B) The multiple-mutation picture. Here, single-mutant, double-mutant, triple-mutant, and quadruple-mutant subpopulations are all present. All the mutations except those happening in the most-fit individuals will be outcompeted because they arise in less-fit individuals; they are thus wasted. As the population evolves, the clones in the less-fit side of the distribution decline, whereas those in the more-fit side grow, and new multiple mutations are added. Thus, the fitness distribution moves toward higher fitness with a steady-state width. This simple picture neglects one-by-one clonal interference by assuming that all mutations confer the same fitness advantage s.

(C) A more complete picture, with both multiple mutations and clonal interference. Each lineage can generate various different mutations, but only the largest (or occasionally a somewhat smaller) such mutation contributes to the long-term evolution (these mutants are shown in blue). These blue mutations are the largest mutations that occur in a typical time before further multiple mutations arise; they thus tend to have some typical size, $\bar{s}$. One-by-one clonal interference and multiple-mutation processes together determine the value of $\bar{s}$, but given $\bar{s}$, the simple multiple-mutation analysis of (B) describes the accumulation of these mutations.

make clear its nature, we refer to it as the successional-fixation regime.

When mutations establish faster than they can fix, different mutations occur and spread through the population concurrently and can interfere with each other (the "Hill-Robertson effect" [28, 29]). This concurrent mutations situation is more complicated than the successional-fixation regime, and various analyses have considered different aspects of the dynamics. One approach (Figure 1A) focuses on competition between mutations that have different fitness effects [20–26]. This has been called "clonal interference" by its creators; we refer to it as "one-by-one clonal interference" because it assumes that mutations fix one at a time. This analysis considers a mutation B with fitness

advantage s_B that becomes established in a population in which a different lineage with mutation A (with fitness advantage s_A) is already spreading. If $s_A > s_B$, the lineage that carries B will be eliminated, whereas if $s_A < s_B$, lineage B can overtake and eliminate A. This process "wastes" some beneficial mutations and thus slows down the speed of evolution. Because more mutations are lost in larger populations, this analysis predicts that v increases slowly as NU_b rises; the details depend on the distribution of the strengths of beneficial mutations, which we call $\rho(s)$.

Although one-by-one clonal interference is one important aspect of the large-NU_b dynamics, there is another crucial feature that affects the evolution of such populations. Even if a more-fit mutation B occurs before an

earlier but less-fit mutation A fixes, A is not always doomed: An individual with mutation A can get an additional mutation C. If the combined fitness of A and C exceeds that of B, mutation A (along with C) can fix after all. One-by-one clonal interference neglects these complications. It assumes that mutations only occur in the majority population ("wild-type") and that the most-fit such mutant outcompetes all others and becomes the new wild-type, and then the process repeats. This is the one-by-one assumption. Yet the creation of multiple mutants is not a small effect: In populations large enough that one-by-one clonal interference is important, double mutants will routinely appear. Thus, considering one-by-one clonal interference alone is incomplete. In typical laboratory yeast and microbial populations, N is often large enough for even triple and quadruple beneficial mutations to regularly occur before the first mutation in the series fixes [30]. Recent simulation studies [31, 32], as well as some experiments [33], have also indirectly hinted at the importance of these multiple mutation effects.

When multiple mutations are common, a different picture of the evolutionary dynamics is necessary. We must consider the competition between mutants that arise in lineages that already have other beneficial mutations. The beneficial mutations that matter most are those that occur in individuals that already have many others. Less-fit individuals that get an additional mutation will usually still be less fit than the most-fit individuals in the population and hence doomed to eventual extinction. This effect also "wastes" beneficial mutations and thus also causes the speed of evolution to increase only slowly as the total beneficial mutation rate NU_b rises.

One-by-one clonal-interference analyses focus on the competition between beneficial mutations arising from their different fitness effects and ignore the competition between mutations based on the fitness of the individual they occurred in. We take here the opposite approach and focus on the effects of multiple mutations accumulating in the same lineage (Figure 1B). Specifically, our "multiple-mutations" analysis considers the possibility that a second beneficial mutation arises in the lineage of an earlier mutation A well before that lineage dominates the population. This creates a new more-fit lineage A*. A further mutation can convert A* into A**, but mutations in individuals other than A* are wasted. This is true even though mutations in A* individuals are much rarer than those in other individuals (in light of the fact that A* individuals are rare), because the mutations that confer a particular benefit in A* are more strongly selected for than mutations that confer the same benefit but occur in less-fit lineages. Mutations in A** then create a still more-fit lineage A***, and so on. This establishment of mutations on top of existing unfixed mutations increases the width of the population fitness distribution (i.e., it increases the variation in fitness). But this tendency is countered by the selection against the remainder of the population, which is less fit than these multiply-mutant individuals; this selection increases the mean fitness of the population and reduces the variation in fitness. Eventually these competing forces balance, creating a steady state shape of the evolving fitness distribution, with the broadening produced by the continuing establishment of mutations balanced by the narrowing by selection. When there is a large supply of possible beneficial mutations, this distribution moves continuously toward higher fitness as it maintains the shape set by the beneficial mutation-selection balance.

As NU_b increases, the fitness distribution gets broader both because multiple mutations happen more quickly and because larger less-fit subpopulations take longer to eliminate. Concomitantly, the evolution gets faster because the speed of evolution is roughly equal to the fitness variance of the population. Our key result is that the speed of evolution and the variance in fitness both increase logarithmically with N and logarithmically with U_b (Box 1)—but not with the combination NU_b. Our analysis is described in much greater detail elsewhere [30].

The results in Box 1 reflect the simplest multiple-mutations model (Figure 1B), which assumes that all mutations have the same effect, $\tilde{s}$, so that one-by-one clonal interference is absent by definition. Others have recently studied similar models in regimes relevant to other situations [34, 35], and earlier work [1–3] took the first steps in the analysis described above but did not correctly account for stochastic effects that control the timing between the establishment of successive mutations or for the balance between mutation and selection.

One-by-one clonal interference and the simplest multiple-mutation analyses are both incomplete. Each neglects the important effect that dominates the other. Neglecting multiple mutations never gives a complete picture of the dynamics because whenever one-by-one clonal interference is important, so are multiple mutations. However, our multiple-mutation analysis can partially account for the effects of one-by-one clonal interference because in many situations, mutations with a small range of fitness effects around some value $\tilde{s}$ dominate the evolution (Figure 1C) [30]. Mutations much smaller than $\tilde{s}$ occur frequently but grow too slowly to interfere with mutations of size $\tilde{s}$ (i.e., they are wasted because of clonal interference with the mutations of size $\tilde{s}$). Unless the distribution of mutational effects $\rho(s)$ falls off very slowly with s (slower than $1/s^3$), mutations much more beneficial than $\tilde{s}$ happen rarely enough to have little overall impact. The multiple-mutation analysis cannot predict $\tilde{s}$ because this depends in a subtle way [30] on the unknown distribution of mutational effects and the resulting clonal-interference processes. However, if we take $\tilde{s}$ as a parameter to fit from experiments, the multiple-mutation theory implicitly accounts for one-by-one clonal-interference effects, provided that we redefine U_b to be the mutation rate toward beneficial mutations of roughly this size. However, if $\rho(s)$ falls off slower than exponentially with s, $\tilde{s}$ will depend significantly on N and U_b, and the behavior is more complicated.

Results and Discussion

Our multiple-mutation analysis predicts that the speed of evolution and the variation in fitness within a population both increase logarithmically with N and with U_b. It also shows that neglecting multiple mutations is a serious flaw of one-by-one clonal-interference analyses.

Box 1. Heuristic Analysis and Predictions of the Multiple-Mutations Theory

In the simple model of multiple mutations of the same effect s, there are two factors that determine the speed of evolution. The first is the dynamics of already established populations, which is dominated by selection. We define the *lead* of the distribution, qs, as the difference between the fitness of the most-fit individual and the mean fitness of the population; the fittest individuals have q more beneficial mutations than the mean. Once it is established, the fittest population grows exponentially, first at rate qs but more slowly as selection increases the mean fitness. Growing from this population's establishment upon reaching approximately $\frac{1}{qs}$ individuals (which is a size it reaches rapidly if it does so at all [B1]) until it reaches a large fraction of N will thus take time $\ln(Nqs)/(\frac{qs}{2})$ (because $\frac{qs}{2}$ is the average growth rate of the mutant relative to the mean growth rate during the period between establishment and fixation), and in this time the mean fitness will increase by qs. Therefore, $v \approx (qs)^2/[2\ln(Nqs)]$.

The other factor is the dynamics of the most-fit subpopulations (the "nose" of the fitness distribution), where new mutations are essential. A more-fit mutant that moves the nose forward by s will be established a time τ_q after the previous most-fit mutant. Thus, the nose advances at a speed $v = s/\langle \tau_q \rangle$, where $\langle \tau_q \rangle$ is the average τ_q. After it is established, the fittest population n_q will grow exponentially at rate qs and produce mutants at a rate $U_b n_q \sim U_b \frac{1}{qs} e^{qst}$. Many new mutants will establish soon after the time τ at which $U_b qs \int_0^\tau n_q(t)dt = 1$, so the time it takes a new mutant to establish is $\tau_q \sim \frac{1}{qs}\ln(s/U_b)$. This means the nose advances at rate $v = s/\langle \tau_q \rangle \sim qs^2/\ln(s/U_b)$. Yet we argued above that the bulk of the population fixes the speed of the mean via the selection pressure: $v \approx (qs)^2/[2\ln(Nqs)]$. In steady state, the speed of the mean must equal the speed of the

nose—the mutation-selection balance. This implies that

$$q \sim \frac{2\ln[Ns]}{\ln[s/U_b]}$$

and

$$v \sim \frac{2s^2\ln[Ns]}{\ln^2[s/U_b]}.$$

This crude argument neglects some important details of the stochastic process at the nose, but the basic qualitative behavior follows from this intuitive reasoning. We present a more detailed and careful analysis (and simulations to test the theory) elsewhere [B2], and find

$$v \approx s^2 \left[\frac{2\ln[Ns] - \ln\left[\frac{s}{U_b}\right]}{\ln^2\left[\frac{s}{U_b}\right]} \right],$$

$$qs \approx \frac{2s\ln[Ns]}{\ln\left[\frac{s}{U_b}\right]}.$$

These are the two key predictions we test in this work. In comparing with experiments, we must also account for transient effects, which lead to slower adaptation before the steady state mutation-selection balance is reached. These transient effects are greater in larger populations; details of this effect are presented elsewhere [B2].

Box References

B1. Otto, S.P., and Barton, N.H. (1997). The evolution of recombination: Removing the limits to natural selection. Genetics *147*, 879–906.
B2. Desai, M.M., and Fisher, D.S. (2007). Beneficial mutation-selection balance and the effect of linkage on positive selection. Genetics, in press.

We set out to test these predictions by evolving asexual populations of diploid budding yeast in glucose-limited media for 500 generations at three different effective population sizes ranging 1400 to 3.5×10^6, each with two different mutation rates: "nonmutator" populations and msh2Δ "mutator" populations with U_b estimated to be ten times higher (G. Lang and A.M., unpublished data; based on the elevation of mutation rate at two particular loci and hence only a rough estimate; see Experimental Procedures). The generation time in this media was initially approximately 130 min, compared to 90 min in rich media.

We periodically measured the fitness of each entire population by mixing a sample of it with a derivative of the ancestral strain that had been labeled with yellow fluorescent protein, growing the mixed population for 20 generations, and determining the ratio of the two strains at the beginning and end of the assay by using flow cytometry to distinguish labeled from unlabeled cells (see Experimental Procedures). The total fitness changes over the 500 generations were used for

obtaining the average speed of evolution (Figure 2A). We also measured the distribution of fitnesses within some of the evolved populations by isolating 96 individuals from each population and then measuring their individual fitnesses (Figure 3).

Our data are clearly inconsistent with the simple successional-fixation prediction, v linear in NU_b (p < 0.001). Other simple interpretations are ruled out by the observed time dependence of the mean fitness of our populations (Figure 2B). The rate of fitness increase is roughly constant, in particular showing no evidence of slowing down as the experiment progresses (if anything, a slight speeding up is seen). This indicates that neither antagonistic epistasis (i.e., the combined effect of two beneficial mutations being less than the sum of their separate effects) nor a limited supply of beneficial mutations (i.e., "running out" of beneficial mutations) can be responsible for the observed weak dependence of v on N. Note that the batch culture environment remains the same throughout our experiment, and the populations are in exponential phase throughout, and
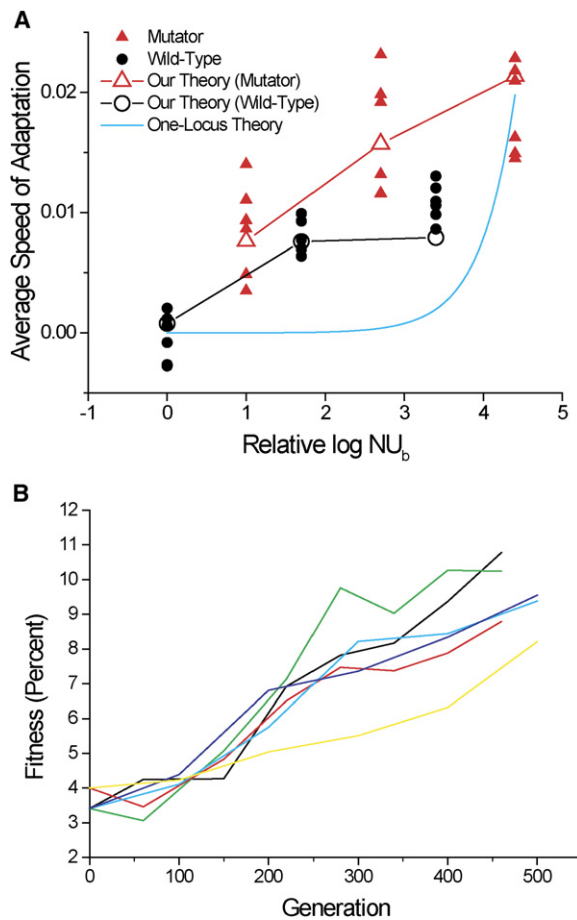
Figure 2. Average Rate and Kinetics of Adaptation

(A) Average speed of adaptation (*v*) of our experimental populations, in percent fitness increase per generation, versus log[NU_b] (scaled to the smallest nonmutator population). *N* is the effective population size (which takes on three values, $N = 1400$, $N = 7 \times 10^4$, and $N = 3 \times 10^6$), and U_b is the beneficial mutation rate. Red triangles represent mutators, and black circles represent nonmutators. The negative adaptation rates of some of the smallest NU_b populations are due to a combination of measurement error and deleterious mutations. Our predictions are obtained from Equation 1 in Box 1, modified to include the initial transient behavior (which causes the "flattening" of our theoretical predictions as *N* increases). Note that our predictions are not a function of the product NU_b but rather are different for mutators and nonmutators with similar NU_b. The one-locus successional-fixation prediction, *v* linear in NU_b, is shown for comparison (blue).

(B) Evolution of the mean fitness, in percent per generation, of the largest mutator populations (six independent lines) through the course of the experiment. The non-zero values at time zero reflect the reduced fitness of the marked reference strain. Note that the rate of fitness increase does not slow down on average over the course of the experiment. Other populations show a similar (although smaller) steady increase in average fitness.

therefore environmental changes cannot explain these results.

Our data are also inconsistent with one-by-one clonal-interference analyses because of their assumption that mutations fix singly in succession. This inconsistency is most apparent for our largest populations. Our large nonmutator populations increased in fitness by approximately 4%–7% in 500 generations. This is not enough time for two or more mutations adding up to 4%–7%

to fix one by one (i.e., successively). For example, two 3.5%-effect mutations would take a minimum of 1000 generations to fix successively; all other combinations adding to 4%–7% would take even longer. A similar argument applies to our large mutator populations.

Thus, if single beneficial mutations fix successively, *one* large such mutation must be responsible for almost the entire observed fitness increase. However, this is also inconsistent with the data. Figure 2B shows that the mean fitness of our populations increases smoothly, and the individual profiles are similar to one another. Both features imply that the evolution is not dominated by single large mutations. If it were, the mean fitness would remain constant for a time and then rapidly increase by the amount of the large mutation. For a 7% mutation, for example, most of the increase in fitness would occur in just 30 generations (fixation times are much longer because mutations are rare for a long time). The fitnesses of different populations would also show a wide range of kinetics depending on whether their large-effect mutations occurred early or late (Figure 4A). Yet this is not at all what we see. Instead, the gradual increase in fitness and similar kinetics between lines strongly suggest that many smaller mutations are steadily accumulating (Figure 4B). This cannot happen unless multiple mutations sweep together: Successional sweeps of small-effect mutations would take far too long (Figure 4C). A more detailed discussion, including other inconsistencies with one-by-one clonal interference and special circumstances in which one-by-one clonal interference could produce the observed results, is presented in the Supplemental Data.

The above arguments suggest that the multiple-mutation analysis is the correct explanation for our results. A key qualitative prediction of this analysis is that the width of the fitness distributions in large populations should be greater than in small populations. In contrast, one-by-one clonal interference predicts that fitness distributions will show pronounced fluctuations over time for any population size: narrow and dominated by a single clone most of the time or, if measured during a selective sweep, clearly bimodal. Similar behavior would arise from a simple successional-fixation (one-locus) analysis, except that the rate of sweeps would increase dramatically in large populations. In actuality, for both mutators and nonmutators, we find that the fitness distributions of large populations are broader than of small ones (Figures 3A–3D).

These predictions can be made quantitative: The expected widths of the fitness distributions and the speeds of evolution are given by the formulas in Box 1. These predictions depend on just two unknown parameters: the typical size of the beneficial mutations responsible for the fitness increase, $\tilde{s}$, and the rate at which these beneficial mutations occur, U_b. One might worry that for any experimental data, there would be a U_b- and-$\tilde{s}$ combination that would produce a good fit. This is not so. In the smallest populations, NU_b is so small that they can only be in the successional-fixation regime. These populations tightly constrain U_b and $\tilde{s}$ in a way that is independent of the multiple-mutation theory, ruling out arbitrary U_b and $\tilde{s}$ that might have yielded good fits to the other data. Within these constraints, we
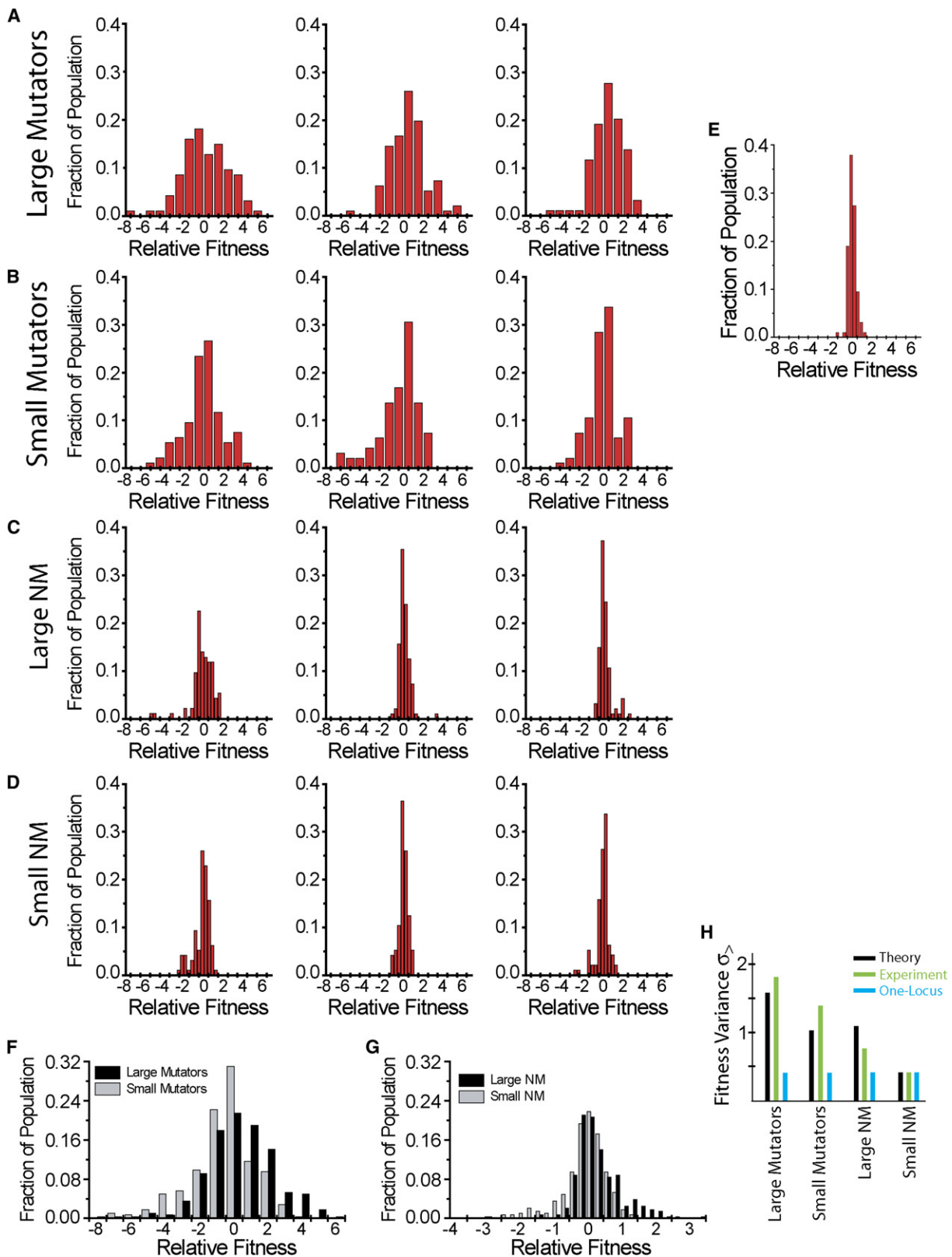
Figure 3. Distributions of Fitnesses within Evolving Populations

(A–D) Fitness distributions of evolved populations after 500 generations, for three independently evolved lines of the following: (A) largest mutator populations, (B) smallest mutator populations, (C) largest nonmutator populations, and (D) smallest nonmutator populations. Fitnesses (in percent per generation) relative to the median of each population are plotted.

(E) The experimental error was estimated by measurement of the fitness of the same clone 96 times: This "error distribution" has SD of 0.4%.

fit U_b and $\tilde{s}$ from the data and find $U_b = 2.4 \times 10^{-4}$ for mutator populations (hence $U_b = 2.4 \times 10^{-5}$ for nonmutators), and $\tilde{s} = 2\%$. Details of the theory-independent constraints and the fit to data are described in the Experimental Procedures. The resulting comparison between theory and experiment is summarized in Figures 2A and 3H. The predicted increases in mean fitness (which give the speeds of evolution shown in Figure 2A) and widths of the fitness distributions are each within a single fitness increment $\tilde{s}$ of the experiments—as accurately as theory could possibly predict. There are, however, small systematic discrepancies: The theory overestimates the mean fitness increases for mutator populations and underestimates their width and makes the opposite errors in nonmutators. This is likely because of deleterious mutations, which we now consider.

Deleterious mutations complicate the shapes of the fitness distributions. However, their effects are most pronounced on the less-fit side of the distributions: On the more-fit side, all the clones are depleted similarly by deleterious mutations, and the modifications of the shape of the distribution are small. Thus, in the analysis described above, we only use the more-fit side, above the median. But deleterious mutations may indirectly affect the more-fit side of the fitness distributions, for example by decreasing the median fitness. They will also cause a reduction in the mean fitness of the population and hence could reduce the observed speed of evolution.

Unfortunately, the effects of deleterious mutations depend on the unknown distribution of their fitness decrements, so precise predictions are impossible. We can, however, estimate their maximum impact by looking at the small population fitness distributions. The small nonmutator fitness distributions are no wider to the right than expected from the measured experimental errors (Figures 3D and 3E); this implies that deleterious mutations do not significantly reduce the mean fitness in nonmutators nor do they affect the above-median fitness distribution width. In other words, the contribution of deleterious mutations in nonmutators is minor and limited to a slight increase in the width of the less-fit tail. In mutators, on the other hand, the width to the right of the median in the small populations could be entirely due to reduction of the median by deleterious mutations, entirely due to beneficial mutations, or due to some combination of the two. This means that in all the mutator populations, deleterious mutations may decrease the mean fitness by at most 2% and broaden their fitness distributions by convolving them (defined in [36]) with a distribution of SD 1.4%. These shifts lead to slight changes in the best-fit U_b and $\tilde{s}$ and thus lead to the opposite shifts in the predicted results for nonmutators. These corrections roughly account for the systematic discrepancies between experiments and the multiple-mutation theory.

Although the multiple-mutation picture better explains our experiments, clonal interference must nevertheless also occur. Mutations of very small effect are certainly being regularly wasted, and this process partially determines the typical size, $\tilde{s}$, of the mutations that dominate the evolution. However, our data indicate that the accumulation of multiple mutations, the effect omitted in one-by-one clonal-interference analyses, is crucial. After fitting $\tilde{s}$ from data to implicitly account for clonal-interference effects, we find that the simple multiple-mutation theory is consistent with our experiments, especially once we consider the additional effects of deleterious mutations.

Several other recent experimental studies have also found that, as in our experiments, the speed of adaptation increases less than linearly with population size and mutation rate [4, 16–19]. This has been taken as support for one-by-one clonal interference. But our multiple-mutations analysis also predicts a specific form of this less than linear dependence on N and U_b, albeit for different reasons. This earlier work is not sufficiently detailed for distinguishing between one-by-one clonal interference and our multiple-mutations model.

If the beneficial mutations of size $\tilde{s} \approx 2\%$ are point mutations, combining the estimate of U_b with the per-base-pair mutation rate of order 10^{-9} per generation [37] suggests that the target size for beneficial mutations in our experiments is a few thousand base pairs. This is substantially greater than the beneficial mutation rates in several earlier studies done in different environments [38, 39] but closer to recent estimates by Joseph and Hall [40]. It is possible that there are several targets of roughly a hundred base pairs such as genes where inactivating one of the two copies in a diploid conveys an advantage, or a number of much smaller mutational hot spots (as found by [41]), whose mutation rate is much higher than the average per-base-pair mutation rate—perhaps having evolved to allow rapid mutational switches between different metabolic environments encountered in the natural history of budding yeast.

Finally, we note that the logarithmic increase in the speed of evolution with N and U_b in the large-NU_b multiple-mutations regime is dramatically slower than the linear successional-mutations regime. The difference has many implications. For example, the potential advantage of sex in combining mutations from different lineages becomes more pronounced in large populations, whereas mutator phenotypes become less useful as population sizes increase.

Experimental Procedures

Experimental-Evolution Protocol

The experimental lines were established from a single W303 diploid with a heterozygous deletion at both *ime1* (required for sporulation) and *msh2* (this deletion elevates the mutation rate). We created the *ime1* deletion by amplifying from plasmid pFA6-kanMX4 with primers F1 (5′-GAAAAA AATAAT AAAAGA AAAGCT TTTCTA TTCCTC TCCCCA CAAACA AAGGTC GACGGA TCCCCG GGTT-3′) and R1 (5′-AATGGA TATATT TTGAGG GAAGGG GGAAGA TTGTAG TACTTT TCGAGA ATCGAT GAATTC GAGCTC GTT-3′); this amplification created a deletion-disruption cassette used to delete *ime1*

(F and G) The distributions at each N and U_b are shifted to a common mode and averaged. Large (black) and small (gray) mutator and nonmutator distributions are shown. Note that the small population distributions are narrower than the large distributions on the more-fit side. On the less-fit side, the small populations are broader than the large, probably because of the longer times available for accumulation of deleterious mutations between beneficial ones.

(H) The widths of the more-fit halves, $\sigma_>$, are compared to our theoretical predictions and the one-locus successional-fixation-theory prediction.
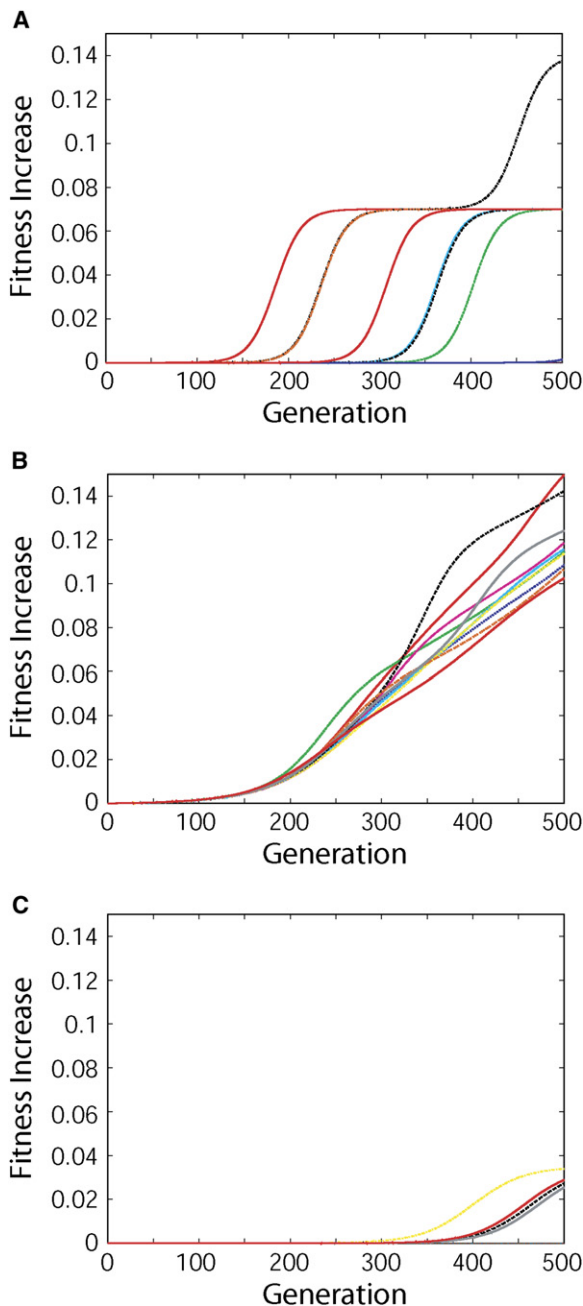
Figure 4. Simulated Kinetics of Adaptation

Computer simulations showing the kinetics of the increase in mean fitness in ten simulated populations of size $N = 3.5 \times 10^6$, the same as our large experimental populations.

(A) Assuming a single 7%-effect mutation is responsible for the evolution ($U_b \sim 10^{-7.5}$). The mean fitness increases in a sharp selective sweep whose timing depends on when the mutation happened to occur. In one line, a second mutation also occurs.

(B) Multiple-mutations kinetics: the accumulation of multiple 2%-effect mutations (with $U_b = 2.4 \times 10^{-4}$). The fitnesses increase smoothly, and different populations behave similarly.

(C) Sequential fixation of small 3.5% mutations. The mutation rate is assumed to be as great as is possible, consistent with not having multiple mutations ($U_b \sim 10^{-7.5}$). In 500 generations, there is barely time for one such mutation to fix; two is impossible.

and replaced *ime1* with *KANmx6*, which confers resistance to G418 [42]. The *msh2* deletion cassette was amplified from plasmid pAG25 with primers F1 (5′-AAAAAT CTCTTT ATCTGC TGACCT AACATC

AAAATC CTCAGA TTAAAA GTGGTC GACGGA TCCCCG GGTT-3′) and R1 (5′-ATCTAT ATATTA TCTATC GATTCT CACTTA AGATGT CGTTGT AATATT AATCGA TGAATT CGAGCT CGTT-3′); this amplification created a deletion-disruption cassette used to delete *msh2* and replaced it with *NAT1*, which confers resistance to Clonat [43]. This resulted in a genotype $\frac{mat\alpha}{mata} \frac{ime1\Delta::KANmx6}{IME1} \frac{msh2\Delta::NAT1}{MSH2} \frac{URA3}{ura3} \frac{CAN1}{can1} \frac{ade2^-}{ade2^-}$. This was sporulated, and the spore clones mated to create two independent homozygous *ime1Δ msh2Δ* "mutators" and two independent homozygous *ime1Δ* "nonmutators." We refer to all these clones as asexuals because they are unable to sporulate. Each genotype was used for founding nine lines, three lines at each of three different effective population sizes, from two independent diploids. All initial lines were approximately clonal. The elevation of U_b in the mutators is impractical to measure because it depends only on the unknown loci where beneficial mutations can occur. We thus assume that mutators have U_b of order ten times that of nonmutators, as indicated by previous measurements of *msh2Δ* cells at CAN1 and URA3 (G. Lang and A.M., unpublished data). This is only a rough estimate, but our theoretical predictions are fairly insensitive to this.

Each initial population was grown overnight in YEPEG (YEP + 2.5% ethanol, 2% glycerol, where YEP is 2% yeast extract, 2% peptone, 0.0025% adenine, and tryptophan) [44] for eliminating possible petite phenotypes and then placed in the selective media at the appropriate bottleneck population size to begin the experiment. Selection was performed in YEP + 0.05% dextrose, ampicillin at 100 μg/mL, and tetracycline at 25 μg/mL (LG). Cultures were grown in 15 ml of LG in 50 ml test tubes and continuously mixed in roller drums at 30° until they reached a density of approximately 1.5×10^7 cells/mL, half the saturation density in this media. Each culture was then counted with a Coulter counter and an appropriate amount of media was transferred to fresh LG. The amounts transferred were chosen for achieving bottleneck population sizes of $N_b = 100$, $N_b = 7100$, and $N_b = 5.5 \times 10^5$.

The differing bottleneck sizes in the same volume of media required different numbers of generations G between transfers, $G \approx 21$, $G \approx 14.5$, and $G \approx 8.5$ for small, medium, and large populations, respectively. This gives effective population sizes separated by factors of 50: $N = 1.4 \times 10^3$, $N = 6.9 \times 10^4$, and $N = 3.5 \times 10^6$ (see below).

The serial dilution process was carried out for approximately 500 total generations of all of the lines. Beginning from the same original starting lines, the entire experiment was then repeated. Aliquots from the evolving cultures were frozen periodically throughout the experiment in LG + 7.5% glycerol.

This experiment was originally intended to compare sexual and asexual populations. Accordingly, all lines were periodically put through sporulation cycles. The asexual lines we discuss in this paper are unable to sporulate but for consistency experienced the same sporulation conditions as sexual lines. In each sporulation cycle, the cells were transferred at 1.5×10^7 cells/mL to YEPA (YEP + 2% potassium acetate) [44]. They were grown in YEPA for 6 hr, then in SPM (2% potassium acetate, 0.02% raffinose, 0.0005% adenine, ampicillin at 100 μg/mL, and tetracycline at 25 μg/mL) [44] for 48 hr, placed on YPD (YEP + 2% dextrose) [44] plates for mating overnight, and then returned to LG. Total growth during this process was approximately two generations. In the first 500-generation experiment, sporulation cycles were carried out every 100 generations. In the second, independent experiment, they were carried out every 60 generations. The fitness distributions shown are all from the latter populations.

Fitness Measurements

To measure fitness, we competed the evolved strains against reference strains. These reference strains were constructed from spores from the original starting line, transformed to create Hygromycin-resistant strains (for colony-counting assays) and a Hygromycin-resistant strain expressing yellow fluorescent protein (YFP, for fluorescence-activated cell sorting (FACS) assays). This reference strain was constructed with a pVENUs plasmid containing YFP linked to a HIS3 marker, generously provided by Kurt Thorn (Bauer Center for Genomics Research, Harvard University). A 1433-bp fragment containing a Hygromycin resistance cassette was obtained by digesting pAG32 with EcoRV and Mlu1. The HIS3 marker was then removed from pVENUs by digestion of this plasmid with EcoRV and Mlu1 for removal of the 1055-bp fragment containing the HIS3 coding

region. The Hygromycin resistance cassette was ligated with the resulting 3671-bp vector fragment containing a YFP coding region for generating pVEN2. We created the Hygromycin-resistant YFP strain by amplifying from pVEN2 with primers F1 (5′-CCGCTG TCGGTA TGGGTG CCGGTG CTCTAG CTGCTG CTGCTA TGTTGT TAGGTC GACGGA TCCCCG GGTT-3′) and R1 (5′-CGAAAA TTTTGA AAAAAG CCATAT AGATAT TATAAA AAATCA GAGATT TCTCGA TGAATT CGAGCT CGTT-3′); this amplification created a cassette used to fuse the YFP, linked to Hygromycin resistance, to *cwp2* [43]. Although Cwp2 is a cell-wall protein, the Cwp2-YFP fusion is cytoplasmic.

For measuring the mean fitness of an evolved population, approximately 10 μl of a reference strain was unfrozen onto a YPD plate and left to grow overnight. These cells were then placed in LG overnight to reacclimate. At the same time, approximately 10 μl of the evolved strain was unfrozen and placed in LG overnight. These two lines were then mixed at a density of order 10^5 cells/mL, and the ratio r_i of the number of reference to evolved individuals was measured. The cells were grown to approximately 1.5×10^7 cells/mL, and then 10 μl of the culture was transferred to new media. They were again allowed to grow and diluted. After growth for a third time to approximately 1.5×10^7 cells/mL (a total of approximately $t = 19$ generations of growth), the ratio of evolved to reference r_f was measured. The fitness difference was defined to be $\Delta s = \frac{1}{t}\ln\left[\frac{r_i}{r_f}\right]$. The fitnesses of the starting lines were simultaneously measured for determining the initial fitness advantage or disadvantage of the reference strain. These were subtracted from the results to yield comparisons between the evolved and starting fitness.

To measure the ratio of reference to evolved populations by colony counting (used for measuring the mean fitness in the first of the 500-generation experiments), we diluted and plated the mixture of the two strains on YPD plates. After individual colonies were visible on the plates, we replica-plated these plates to YPD and Hygromycin plates (YPD + Hygromycin B at 300 μg/mL [43]) and counted the number of Hygromycin-resistant reference individuals and Hygromycin-sensitive evolved individuals. These counts were done in replicate on four plates, to give a total of 500–800 colonies counted. For measuring the ratio by FACS (used for all other measurements), an aliquot of the mixture of the two strains was washed out of LG, placed in PBS, sonicated, and then analyzed with a MoFlo FACS machine (DakoCytomation, Carpinteria, CA). Five thousand to one hundred thousand cells per mixture were analyzed. The cells clearly divide into YFP-labeled and unlabeled individuals and thus yield the ratio of reference to evolved cells.

To measure the fitness distribution within a population, we unfroze that population and diluted and plated it to single colonies on a YPD plate. Ninety-six randomly chosen individual colonies were picked from this plate and placed in LG overnight to reacclimate. These were then mixed with a reference strain (also plated and placed in LG to reacclimate overnight), and the fitness measurements proceeded as above.

Fits to Theoretical Results
The less-fit sides of the fitness distributions are heavily influenced by deleterious mutations. These bias the shapes, particularly of this side of the distributions. In addition, we occasionally observe a single individual 8%–10% less fit than the mean, presumably because of a large-effect deleterious mutation. This means that the standard deviation, or any other statistic that depends on the whole distribution, can be heavily influenced by deleterious mutations. Therefore, in making statistical comparisons between fitness distributions and with theory, we use only the more-fit half of each distribution. We define the center of the distribution to be the median, x_m, (which is less influenced by outlying deleterious mutations than the mean) and use the second moment to the right of the median, $\sigma_>^2 = \frac{2}{M}\sum_i (x_i - x_m)^2$, as a measure of the width (where x_i are the fitnesses of the $M/2$ measurements above the median). To test the theory, we compare values of $\sigma_>$ between large and small populations at the same mutation rate. Other measures of the width give similar results.

In the parameter ranges relevant for this experiment, the theory predicts an approximately Gaussian fitness distribution (except in the tails where the number of individuals is too small to be sampled anyway). This means we can relate the theoretical q (see Box 1) to the observed $\sigma_>^2$ by $\text{Erfc}\left[\frac{(q-1)s}{\sigma_>\sqrt{2}}\right] = \frac{2}{N(q-1)s}$ in fitting to the multiple-

mutation theory. The lead of the distribution is much greater in a large population than a small one given the same $\sigma_>$ because 1% of a large population represents many more individuals than 1% of a small population. Thus, the difference of the leads between large and small populations is much greater than the difference in $\sigma_>$.

To fit the theory to the data, we calculated the mean speeds of adaptation and leads of fitness distributions from our experiments and estimated the standard error in these values from the interline variation. We defined the best-fit values of $\bar{s}$ and U_b to be those that minimized the squared deviations of the theoretical predictions from the experimental values, measured in units of the standard errors. This fit was done within the constraints imposed by the smallest NU_b populations. These constraints depend only on bounding arguments and are independent of the multiple-mutation theory. The one-locus theory result is an upper bound on the speed of evolution at given parameters. Thus, if we assume that the smallest mutator populations are in the one-locus regime, for these populations to have evolved as much as observed implies an estimated lower bound on U_b and s (we cannot use the smallest nonmutator populations because these are consistent with not having acquired any beneficial mutations at all). This implies that in order to achieve the mean fitness gains seen in the small mutator populations, and to explain the between-line variations, U_b in mutators must be at least of order $10^{-4.5}$ and $\bar{s}$ must be at least approximately 0.01. At the same time, the smallest NU_b populations evolved by at most a few percent. This sets an upper bound on $\bar{s}$ of a few percent, and given the lower bound on s, it also implies that U_b in mutators is at most of order $10^{-3.5}$. Because the multiple-mutation theory depends only logarithmically on U_b, this factor-of-ten range of U_b is a tight constraint.

There is no single effective population size relevant for comparison to theory. Rather, the population size enters in two ways: the time it takes selection to change the mean fitness and the rate at which new mutations establish. The harmonic mean of the population size is relevant for the former, and Wahl and Gerrish [45] found that the effective size $N = N_b G \ln 2$ determines the latter. Only the latter is relevant for single-locus dynamics because here fixation times are negligible. The two definitions are very similar for all comparisons to our theory made in this paper (these comparisons depend only logarithmically on N), and therefore we use the latter formula throughout and neglect the difference. For the discussion of the inconsistency with clonal interference, we use the harmonic mean effective population size where appropriate (i.e., when discussing fixation times).

References

1. Crow, J.F., and Kimura, M. (1965). Evolution in sexual and asexual populations. Am. Nat. *909*, 439–450.
2. Maynard Smith, J. (1968). Evolution in sexual and asexual populations. Am. Nat. *102*, 469–473.
3. Maynard Smith, J. (1971). What use is sex? J. Theor. Biol. *30*, 319.
4. Colegrave, N. (2002). Sex releases the speed limit on evolution. Nature *420*, 664–666.

5. Otto, S.P., and Lenormand, T. (2002). Resolving the paradox of sex and recombination. Nat. Rev. Genet. *3*, 252–261.

6. Tenaillon, O., Le Nagard, H., Godelle, B., and Taddei, F. (2000). Mutators and sex in bacteria: Conflict between adaptive strategies. Proc. Natl. Acad. Sci. USA *97*, 10465–10470.

7. Barton, N.H., and Otto, S.P. (2005). Evolution of recombination due to random drift. Genetics *169*, 2353–2370.

8. Barton, N.H. (1995). Linkage and the limits to natural-selection. Genetics *140*, 821–841.

9. Otto, S.P., and Barton, N.H. (1997). The evolution of recombination: Removing the limits to natural selection. Genetics *147*, 879–906.

10. Otto, S.P., and Barton, N.H. (2001). Selection for recombination in small populations. Evolution Int. J. Org. Evolution *55*, 1921–1931.

11. Cox, E.C., and Gibson, T.C. (1974). Selection for high mutation rates in chemostats. Genetics *77*, 169–184.

12. LeClerc, J.E., Li, B.G., Payne, W.L., and Cebula, T.A. (1996). High mutation frequencies among *Escherichia coli* and *Salmonella* pathogens. Science *274*, 1208–1211.

13. Sniegowski, P.D., Gerrish, P.J., and Lenski, R.E. (1997). Evolution of high mutation rates in experimental populations of *E. coli*. Nature *387*, 703–705.

14. Taddei, F., Radman, M., Maynard-Smith, J., Toupance, B., Gouyon, P.H., and Godelle, B. (1997). Role of mutator alleles in adaptive evolution. Nature *387*, 700–702.

15. Giraud, A., Matic, I., Tenaillon, O., Clara, A., Radman, M., Fons, M., and Taddei, F. (2001). Costs and benefits of high mutation rates: Adaptive evolution of bacteria in the mouse gut. Science *291*, 2606–2608.

16. Arjan, J.A., Visser, M., Zeyl, C.W., Gerrish, P.J., Blanchard, J.L., and Lenski, R.E. (1999). Diminishing returns from mutation supply rate in asexual populations. Science *283*, 404–406.

17. Miralles, R., Moya, A., and Elena, S.F. (2000). Diminishing returns of population size in the rate of RNA virus adaptation. J. Virol. *74*, 3566–3571.

18. Miralles, R., Gerrish, P.J., Moya, A., and Elena, S.F. (1999). Clonal interference and the evolution of RNA viruses. Science *285*, 1745–1747.

19. de Visser, J.A.G.M., and Rozen, D.E. (2005). Limits to adaptation in asexual populations. J. Evol. Biol. *18*, 779–788.

20. Gerrish, P. (2001). The rhythm of microbial adaptation. Nature *413*, 299–302.

21. Johnson, T., and Barton, N.H. (2002). The effect of deleterious alleles on adaptation in asexual populations. Genetics *162*, 395–411.

22. Gerrish, P., and Lenski, R. (1998). The fate of competing beneficial mutations in an asexual population. Genetica *102/103*, 127–144.

23. Wilke, C.O. (2004). The speed of adaptation in large asexual populations. Genetics *167*, 2045–2053.

24. Kim, Y., and Stephan, W. (2003). Selective sweeps in the presence of interference among partially linked loci. Genetics *164*, 389–398.

25. Campos, P.R.A., and De Oliveira, V.M. (2004). Mutational effects on the clonal interference phenomenon. Evolution Int. J. Org. Evolution *58*, 932–937.

26. Orr, H.A. (2000). The rate of adaptation in asexuals. Genetics *155*, 961–968.

27. Johnson, T., and Gerrish, P.J. (2002). The fixation probability of a beneficial allele in a population dividing by binary fission. Genetica *115*, 283–287.

28. Hill, W.G., and Robertson, A. (1966). Effect of linkage on limits to artificial selection. Genet. Res. *8*, 269–294.

29. Felsenstein, J. (1974). The evolutionary advantage of recombination. Genetics *78*, 737–756.

30. Desai, M.M., and Fisher, D.S. (2007). Beneficial mutation-selection balance and the effect of linkage on positive selection. Genetics, in press.

31. Yedid, G., and Bell, G. (2001). Microevolution in an electronic microcosm. Am. Nat. *157*, 465–487.

32. Bachtrog, D., and Gordo, I. (2004). Adaptive evolution of asexual populations under Muller's ratchet. Evolution Int. J. Org. Evolution *58*, 1403–1413.

33. Shaver, A.C., Dombrowski, P.G., Sweeney, J.Y., Treis, T., Zappala, R.M., and Sniegowski, P.D. (2002). Fitness evolution and the rise of mutator alleles in experimental escherichia coli populations. Genetics *162*, 557–566.

34. Rouzine, I., Wakeley, J., and Coffin, J.M. (2003). The solitary wave of asexual evolution. Proc. Natl. Acad. Sci. USA *100*, 587–592.

35. Kim, Y., and Allen Orr, H. (2005). Adaptation in sexuals vs. asexuals: Clonal interference and the Fisher-Muller model. Genetics *171*, 1377–1386.

36. Feller, W. (1968). An *Introduction to Probability Theory and Its Applications* (New York: Wiley and Sons).

37. Drake, J.W. (1991). A constant rate of spontaneous mutation in DNA-based microbes. Proc. Natl. Acad. Sci. USA *88*, 7160–7164.

38. Lenski, R.E., Rose, M.R., Simpson, S.C., and Tadler, S.C. (1991). Long-term experimental evolution in escherichia-coli.1. adaptation and divergence during 2,000 generations. Am. Nat. *138*, 1315–1341.

39. Zeyl, C., Vanderford, T., and Carter, M. (2003). An evolutionary advantage of haploidy in large yeast populations. Science *299*, 555–558.

40. Joseph, S.B., and Hall, D.W. (2004). Spontaneous mutations in diploid *Saccharomyces cerevisiae*: More beneficial than expected. Genetics *168*, 1817–1825.

41. Dunham, M.J., Badrane, H., Ferea, T., Adams, J., Brown, P.O., Rosenzweig, F., and Botstein, D. (2002). Characteristic genome rearrangements in experimental evolution of *Saccharomyces cerevisiae*. Proc. Natl. Acad. Sci. USA *99*, 16144–16149.

42. Wach, A., Brachat, A., Pohlmann, R., and Philippsen, P. (1994). New heterologous modules for classical or pcr-based gene disruptions in *Saccharomyces cerevisiae*. Yeast *10*, 1793–1808.

43. Goldstein, A.L., and McCusker, J.H. (1999). Three new dominant drug resistance cassettes for gene disruption in *Saccharomyces cerevisiae*. Yeast *15*, 1541–1553.

44. Sherman, F., Fink, G., and Lawrence, C. (1974). *Methods in Yeast Genetics* (Cold Spring Harbor, NY: Cold Spring Harbor Laboratory Press).

45. Wahl, L.M., and Gerrish, P.J. (2001). The probability that beneficial mutations are lost in populations with periodic bottlenecks. Evolution Int. J. Org. Evolution *55*, 2606–2610.